Modification of a Polycrystalline Gold Electrode by Thiolated Calix[4]arene and Undecanethiol: Self-assembly Process versus Electrochemical Deposition

Barbora Šustrová[1,2], Karel Štulík[1,2], Vladimír Mareček[1]*

[1] J. Heyrovský Institute of Physical Chemistry of AS CR, v.v.i., Dolejškova 3, CZ-182 23 Prague 8, Czech Republic
[2] Charles University in Prague, Faculty of Science, Department of Analytical Chemistry, Hlavova 2030/8, 128 43 Prague 2, Czech Republic
[*] E-mail: barbora.sustrova@jh-inst.cas.cz

Modification of the surface of a polycrystalline gold substrate with thiol compounds has been studied in order to evaluate the possibilities of designing ion-selective electrochemical sensors on this basis. The results of detailed voltammetric and impedance measurements, obtained with gold surfaces modified by self-assembly procedures and by electrochemical deposition of the modifiers are thoroughly discussed and critically compared with those published in the literature. It can be concluded that there are certain possibilities of selective measurements in these systems, but that the spatial heterogeneity of the polycrystalline gold surface seriously limits the applicability and reliability of the system. Therefore, it is expected that substantially better results will be obtained with single-crystal gold substrates and the study in this direction is in progress.

1. INTRODUCTION

The fabrication of self-assembled monolayers (SAMs) on electrode surfaces has become an important area of research utilized in various branches of science. Surface modification of electrodes

provides a useful way for designing ion-selective sensors or immunosensors with high selectivities, and it is an important tool for studies of the membrane transport processes and their kinetics [1-4].

Self-assembly processes on some surfaces, namely those of platinum, mercury, silver or iron, have been described in detail, but the modification of gold electrodes by alkenethiols has probably been studied most widely [1-8].

The principle of self-assembling is spontaneous formation of a modifier molecule monolayer on a solid surface, the modifier molecules being amphiphilic in their character [9]. Specifically in the case of a thiol − gold surface reaction, this principle may be formally considered as an oxidative addition of the S-H bond to gold, followed by reductive elimination of the hydrogen (reaction 1).

$$RSH + Au \rightarrow RS - Au + H^+ + e^- \tag{1}$$

The self-assembly deposition is usually described as a three step process. The first, fastest step is the adsorption of the thiol on the gold surface and the formation of an Au-S bond. The second step involves straightening of the alkyl chains and the third stage, which is the slowest, has been attributed to a reorientation of the terminal groups [10]. The SAM stability and the velocity of the monolayer formation can be influenced by various factors, such as the length of the alkyl chain, or the temperature or the solvent used [11]. Paik et al. [12,13] described the influence of dissolved oxygen or a redox couple on the self-assembly process and explained the effect by assuming that the electrons generated by adsorption reaction (1), which retard the further reaction of thiols with the electrode surface, are consumed by dissolved oxygen or by the redox couple.

In contrast to the spontaneous self-assembly process stands the electrochemical modification of the electrode surface caused by an applied potential. The reasons for potential-assisted modification of an electrode surface may lie in acceleration of the modifying process, in improvement of the SAM quality and in the possibility to control the ratio of the components in a model binary SAM [14]. The potential-assisted deposition process has been described in the literature as an electrochemical anodic reaction where the metal surface is oxidized and a metal − sulfur bond is formed [12-17]. On the other hand, Rohwerder et al. [18] studied the deposition process at cathodic electrode potentials. The adsorption process was slowed down significantly, because a disordered film with a low concentration of thiol molecules was formed first, followed by the formation of an ordered thiol layer and this took a time three orders of magnitude longer than that observed at potentials near the point of zero charge.

Ron at al. [19] assume that the gold oxides formed on the gold electrode surface at a positive potential applied are simultaneously reduced by ethanol and that the thiolated compounds are subsequently adsorbed on the bare gold surface. Accordingly, the gold corrosion, limited by the surface oxide formation, may act as a surface cleaning process [16].

Finally, no effect of the presence of electrolytes on the alkanethiol adsorption has been observed [20], however, the process is affected by the pH value. The adsorption reaction is retarded by a high concentration of hydronium ions in an acid solution [12,17,21].

Although the most frequently used material in electrochemical determination of organic (e.g. [22-34]) as well as inorganic (e.g. [35-45]) compounds under physiological conditions is mercury in liquid form or in the form of amalgam, gold belongs to the traditional electrode materials used in electrochemistry too (in the form of mono-crystalline, poly-crystalline, composite or amalgam electrodes which have been frequently used in the electrochemical detections of various compounds too, e.g., [35,36,46,47]). The present paper describes our research in the field of modification of gold electrode surfaces by thiolated compounds, aimed at designing an ion selective sensor [48,49].

Calixarenes belong to the ionophores, i.e., lipid-soluble molecules which are able to transport ions across the lipid bilayer of the cell membrane. Ionophores have been frequently used for explanation or simulation of real transporting processes of metals, their ions and other species across the cell membranes (phospholipid monolayers and bilayers) [50-58]. Therefore, it is necessary to elucidate the factors influencing these transporting processes, e.g. presence of low molecular weight organic acids, pH [55,59-62]. It is well known that the electrochemical methods have proved many times to be very suitable for investigation of various environmental problems (e.g., [63-72]) as well as in the characterization and description of these processes, mainly voltammetry and electrochemical impedance spectroscopy (EIS) [21,48,49,59].

Two different deposition processes are compared, namely, spontaneous self-assembly and an electrochemically induced deposition at various applied potentials. Thiolated calix[4]arene ($C_4A-(SH)_4$) with 4 –SH groups located on the lower rim and the linear-chain undecanethiol ($C_{11}SH$) (Fig. 1) are used in this study. The optimum adsorption conditions for individual deposition processes of both the species are determined from the reduction desorption peaks and the properties of the modifying layers are studied by electrochemical measurements in simple redox systems.
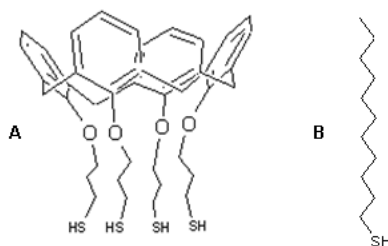
Figure 1. The structures of the calix[4]arene molecule substituted by four –SH functional groups on the lower rim A) and of undecanethiol B) [21].

2. EXPERIMENTAL PART

2.1. Chemicals

The following chemicals have been used throughout: 1.00 μm α-alumina and 0.05 μm γ-alumina (Buehler, USA); sulfuric acid (H_2SO_4 96 % p.a.), ammonia (25%) (Lach-Ner, s.r.o., Czech Republic); sodium hydroxide 1-hydrate (NaOH .H_2O, Suprapur, Merck); lithium perchlorate ($LiClO_4$

p.a, Sigma-Aldrich); acidum aceticum (99% p.a.), potassium ferrocyanide ($K_4[Fe(CN)_6]$ 99.5 % p.a.), (Penta, Czech Republic); tetrabutylammonium hexafluorophosphate (Bu_4NPF_6, 99 %), tetrabutylammonium chloride (TBACl 98%), ferrocene (98%), dimethylformamide (DMF 99.8% v/v), nitrobenzene (99.5% v/v) all from Sigma-Aldrich). Ethanol (96% v/v, Lach-Ner, s.r.o., Czech Republic) was used without further purification. Deionized water (conductance: <0.1 μS cm^{-1}, GORO system, Czech Republic) was used to prepare the aqueous solutions. High purity nitrogen was used for deaeration of the solutions.

The calix[4]arene (C_4A-$(SH)_4$) substance was kindly prepared at the Department of Organic Chemistry, Institute of Chemical Technology (Prague, Czech Republic) and undecanethiol ($C_{11}SH$ 98 %) was purchased from Sigma-Aldrich.

2.2 Instrumentation

The polycrystalline gold disk-working electrode 1 mm in diameter purchased from the Elektrochemické Detektory Ltd. (Czech Republic) and a platinum wire auxiliary electrode have been used in all the measurements. A saturated calomel electrode (SCE, Elektrochemické Detektory Ltd. Czech Republic) has been used as a reference electrode for the aqueous electrolytes. An Ag/AgCl electrode in a 0.01 M TBACl aqueous solution has been used as a reference electrode for the measurements in the organic electrolyte.

Each cyclic voltammogram was recorded after 10 min of continuous stirring and degassing with nitrogen; the stirring was stopped during the measurements. The scan-rate was 0.1 V s^{-1}, for all the supporting electrolytes and the potential ranges are specified in the appropriate paragraphs.

Cyclic voltammetry (CV) and electrochemical impedance measurements (EIS) (5 mV perturbation sine-wave signal, frequency range 100 000 - 0.05 Hz with 5 points per decade) were performed using an Electrochemical Workstation CHI660C (IJ Cambria Scientific, UK) with a CHI660C software.

2.3. Modification of the gold surface

The gold electrode was prepared for modification by mechanical polishing with suspensions of 1.00 μm and then 0.05 μm alumina particles, then electrochemically pretreated by potential cycling in 0.1 M H_2SO_4 within an interval from +1.4 V to -0.6 V (scan rate, 0.5 V s^{-1}, 50 cycles)/ or in 0.01 M $LiClO_4$ ethanolic solution within an interval from -2.0 V to 2.0 V (scan rate, 0.5 V s^{-1}, 50 cycles) if a modification proceeded in the same electrolyte. Finally, the electrode was dried in the nitrogen stream prior to each adsorption process.

Two ways of electrode modification were compared:
A) In the self-assembly process, a volume of 2 μl of the thiol solution (DMF solvent) was directly applied to the clean electrode surface.

B) The potential-assisted deposition was performed using two different electrolytes with dissolved thiol compounds under different potential conditions:

1) 0.1 M NaOH dissolved in a 1:1 mixture of water and ethanol where the modifier was deposited at negative applied potentials,

2) 0.01 M LiClO$_4$ ethanolic solution where the adsorption was in the positive potential range [14-16,19].

The electrode with a deposited thiol layer was washed with ethanol and with distilled water.

The coverage of the modified electrode surface was determined from the voltammetric reduction peak area in the 0.1 M NaOH aqueous solution.

2.4. Electrochemical measurements in redox systems

The simple redox systems of 1 mM K$_4$[Fe(CN)$_6$] in 0.5 M acetate buffer and 1 mM ferrocene in 10 mM Bu$_4$NPF$_6$ dissolved in nitrobenzene were utilized to study compactness of the modifying layers.

Cyclic voltammetry measurements were performed under these conditions:

A) For the K$_4$[Fe(CN)$_6$], the scan started at the initial potential (E$_{In}$), -0.8 V vs. SCE in the positive direction toward the maximum potential (E$_H$), 1.2 V, and then was reversed towards the low potential (E$_L$). The scan rate was 0.1 V·s^{-1}.

B) For the ferrocene redox system, the scan started at E$_{In}$ (= E$_L$) of 0.15 V vs. Ag/AgCl reference electrode and continued in the positive direction to the E$_H$ value of 0.95 V and back, at a scan rate of 0.05 V s^{-1}.

3. RESULTS AND DISCUSSION

3.1. Voltammetric and impedance monitoring of thiol reductive desorption

Cyclic voltammograms obtained with the bare gold electrode and the C$_4$A-(SH)$_4$ and C$_{11}$SH modified electrodes in 0.1 M NaOH aqueous solutions are shown in Fig. 2. The C$_{11}$SH substance is reduced close to a potential of -1.35 V (vs. SCE) and the reduction peak of C$_4$A-(SH)$_4$ is observed close to a potential of -1.45 V (vs. SCE). Nevertheless, another small reduction peak was observed with both the thiol compounds around -1.2 V. Calvente et al. [73] have described this phenomenon as desorption of thiol molecules adsorbed in different energy states, namely, a less stable standing-up position and a more stable laying-down position. Our results disagree with this hypothesis. At a longer time, the thiol layer becomes more ordered when the molecules are in the standing-up position. Therefore, the first reduction peak close to -1.2 V, should increase with increasing adsorption time (t$_{ADS}$), but in our measurement the height (charge) is constant, see Fig. 3, the lower curve.

Another view concerning this phenomenon is provided by the studies of the crystallographic structure of polycrystalline gold [74-77]. Buess-Herman et al. [78] have studied the influence of the crystallographic orientations of gold substrates (polycrystalline gold and gold single crystals with low-index faces) on the values of the reductive desorption peak potential of three different thiols, concluding that the polycrystalline gold surface contains more faces of distinct crystallographic orientation. Therefore, the negative potential scan of the thiol desorption process reveals several reduction peaks. This conclusion agrees better with our results. The authors have further described the influence of the lateral interactions between the adsorbates, stabilizing the monolayer and shifting the reductive desorption potential to more negative values. Moreover, Walczak et al. [77] point out that the adsorbed molecules are bound to the terrace and to the step sites of the terraced gold surface with different binding energies and thus a greater number of reduction peaks appear on the voltammetric curves. The literature also describes the influence of the thiol chain length on the reduction peak position [14,73]. All these studies can explain the differences in the varying reduction potentials of $C_4A\text{-}(SH)_4$ and $C_{11}SH$ on the polycrystalline gold electrode observed by us (Fig. 2).
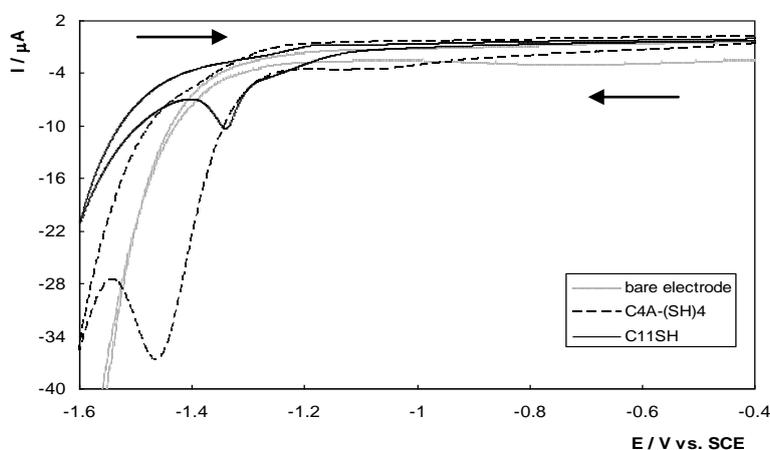
Figure 2. Cyclic voltammograms for reduction desorption of $C_{11}SH$ (solid line) and $C_4A\text{-}(SH)_4$ (dashed line) from a polycrystalline gold electrode surface in 0.1 M NaOH aqueous solution (Initial potential: $E_{In} = -0.4$ V, Lower potential: $E_L = -1.6$ V, $v = 0.1$ V s^{-1}). Self-assembly modification (thiols concentration: c_{ADS} $5 \cdot 10^{-5}$ M in DMF solution; adsorption time; t_{ADS} 10 min for both compounds).

The main reduction peaks at -1.45 V for $C_4A\text{-}(SH)_4$ and at -1.35 V for $C_{11}SH$, which can be attributed with certainty to the reductive desorption of thiols from the most commonly occurring faces on polycrystalline surface (Au (100) terraces), were utilized to determine the optimum adsorption conditions.

The dependences of the reduction peak heights on the potential scan rate have been employed to describe the surface desorption reactions of the two compounds. With $C_{11}SH$, this dependence is

linear (Fig. 4), indicating that the surface adsorption process is predominant. The dependence for C_4A-$(SH)_4$ (not depicted) is also controlled by adsorption, but the reduction peak is less pronounced because of a higher background signal at more negative potentials.
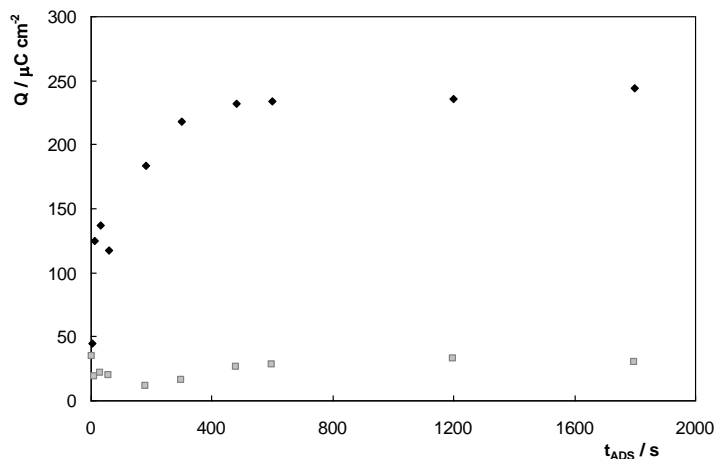
Figure 3. Dependences of the areas of the C_4A-$(SH)_4$ reduction desorption peak (upper curve) and the pre-peak (bottom curve) on the deposition time. Adsorption: Electrodeposition from NaOH 1:1 EtOH:H_2O solution, adsorption time: t_{ADS} = change, thiols concentration: c_{ADS} 12.5 mM, adsorption potential: E_{ADS} = -1.3 V.
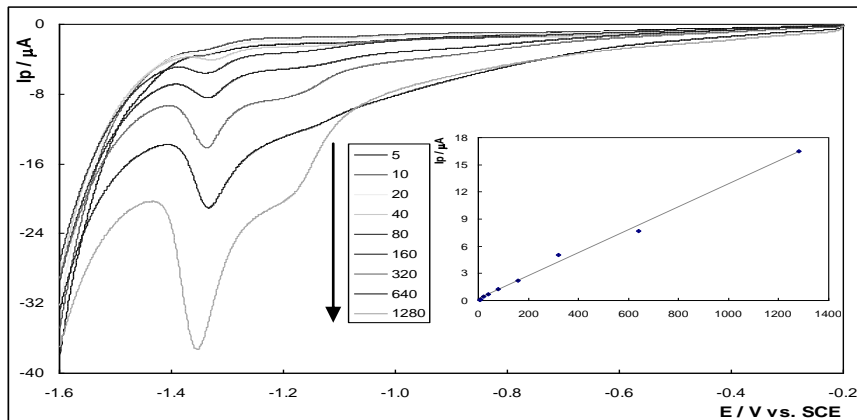
Figure 4. The dependences of the reduction desorption process of $C_{11}SH$ in 0.1 M NaOH on the potential scan rate. (CV: E_{In} = -0.2 V, E_L = -1.6 V). Self-assembly modification (thiol concentration: c_{ADS} $5 \cdot 10^{-5}$ M in DMF solution; adsorption time: t_{ADS} 10 min).

There are also differences in the reduction behavior of the two thiols during repeated voltammetric reduction scans. At high scan rates, over 80 mV s^{-1}, the adsorbed molecules of the two thiol compounds seem to be not completely desorbed from the gold surface. The reduction peak of the

adsorbed molecule is also observed in the subsequent potential scan. This phenomenon is more pronounced for the reduction of $C_{11}SH$, where the peak area in the second reduction scan amounts to about 95 % of that obtained in the first reduction scan, compared to $C_4A\text{-}(SH)_4$, where this value is only around 4 %. This indicates that the desorbed molecules of $C_{11}SH$ immediately form insoluble multiagregate layer close to the electrode surface and the subsequent process of adsorption is faster than the diffusion of the $C_{11}SH$ molecules into the solution.

In the reverse oxidation scan, a small wave is always observed at a distance of 140 mV from the reduction peak (with both the compounds), its area is constant in the two subsequent oxidation scans and this effect is again more pronounced with $C_{11}SH$. This oxidation wave probably corresponds to adsorption of the desorbed thiol molecules, but the shape and height of the wave indicate that the process is very slow and probably takes place during the whole process of the electrode oxidation.

The changes in the double layer capacity (C_{dl}) have been determined for the reductive desorption of adsorbed $C_4A\text{-}(SH)_4$, $C_{11}SH$ (Fig. 5). The impedance spectra have been fitted by a simple Randles circuit consisting of the electrolyte resistance (R_s) in series with an RC parallel circuit (Fig. 5A).
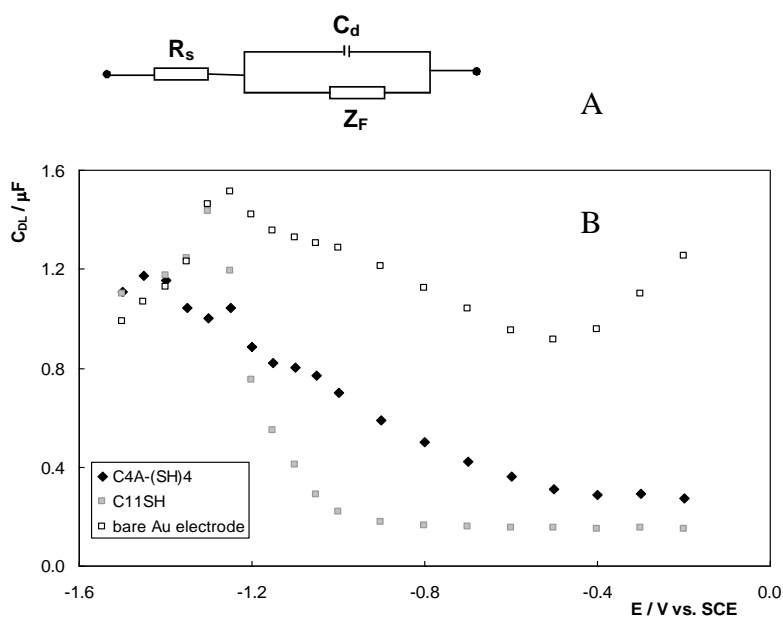
Figure 5. Electric equivalent circuits used to fit the impedance spectra (A) and the changes in the double-layer capacitance during the desorption processes of $C_4A\text{-}(SH)_4$ and $C_{11}SH$, compared to the bare gold electrode (B). Modified electrode: Self-assembly modification (thiols concentration: c_{ADS} $5 \cdot 10^{-5}$ M in DMF solution; adsorption time: t_{ADS} 10 min for both compounds).

The C_{dl} dependences on the electrode potentials indicate that the $C_{11}SH$ layer behaves as an insulator in the potential range from -0.2 to -0.9 V; the capacitance is by an order of magnitude lower

than that of the bare Au electrode surface. Close to a potential of -1.0 V, the C_{dl} value of the $C_{11}SH$ modified electrode begins to increase and at a potential of -1.3 V it corresponds to the bare electrode capacitance. This can be explained by complete desorption of the adsorbed molecules. In comparison, the double-layer capacity of the $C_4A-(SH)_4$ layer is lower than that of the bare Au electrode, but not as low as in the case of the $C_{11}SH$ modified electrode and the character of the capacitance dependence on the potential is the same as that observed on the bare electrode. It indicates that the base electrolyte ions penetrate in some extent through the $C_4A-(SH)_4$ layer to the electrode surface. It can be concluded that the $C_4A-(SH)_4$ layer forms a barrier on the electrode surface, which is stable up to the potential -1.40 V. Nevertheless, the $C_4A-(SH)_4$ layer is not so compact as that obtained in the case of $C_{11}SH$.

3.2. Self-assembly modification

The most common self-assembly process was studied first. Fig. 6 depicts the dependences of the charges on the $C_{11}SH$ modified electrodes on the adsorption time, for three thiol concentrations; similar dependences were obtained for $C_4A-(SH)_4$ (not included). The dependences indicate that the thiol concentration, $5 \cdot 10^{-5}$ M in DMF, appears to be the most convenient for both the thiols. It can be seen that the charge rapidly increases in the beginning of accumulation and then remains stable after a longer adsorption time. Apparently, the S-Au bonds are formed very rapidly, but the ordering of the adsorbed molecules takes a substantially longer time.
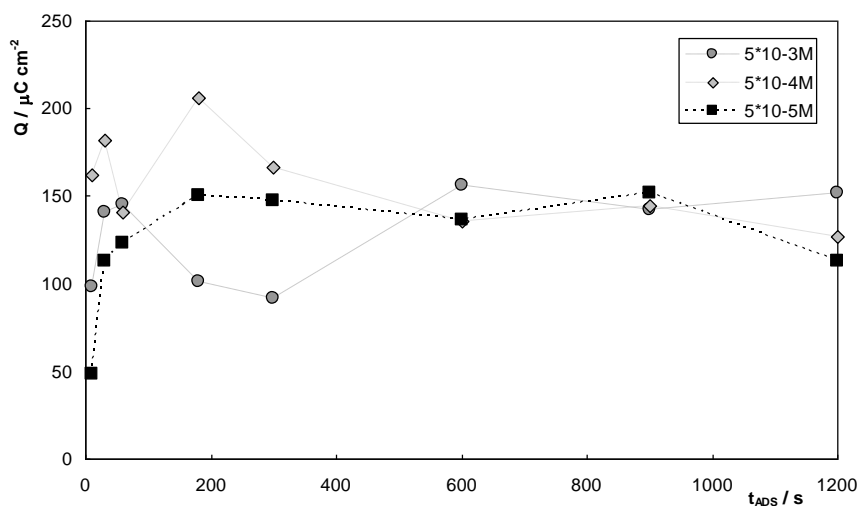
Figure 6. Dependences of the modified electrode charge on the adsorption time and on the concentration of the $C_{11}SH$ during the self-assembly process of modification.

The optimum adsorption time for the self-assembly process of $C_4A-(SH)_4$ is around 10 min. Compared to this, the optimum adsorption time for the deposition of $C_{11}SH$ is close to 4 min. The

electrode surface area corresponding to one modifier molecule, A_{molec}, (Tab.1) has been calculated from the electrode desorption charge.

The area per the $C_{11}SH$ molecule, 0.11 nm^2, corresponds to that found in the literature [78] for similar molecules. This indicates that the compact layer is formed on the electrode surface. On the other hand, the area per the C_4A-$(SH)_4$ molecule, 0.22 nm^2, is five times lower than expected from the literature (1.1 nm^2) [79,80]. It must be emphasized that the C_4A-$(SH)_4$ molecule used in our work is without any substituent on the upper rim, in contrast to the literature data.

3.3. Potential-controlled modification

The potential-controlled deposition of thiols was performed using two different systems, an alkaline 0.1 M NaOH 1:1 water-ethanol solution at negative applied potentials, and a neutral ethanol solution of 0.01 M $LiClO_4$ at positive potentials. The optimum adsorption conditions for these potential-assisted depositions and for the self-assembly process are summarized in Table 1.

The optimum adsorption potential for electrodeposition of C_4A-$(SH)_4$ from 0.1 M NaOH equals -1.3 V, which is somewhat lower than that for $C_{11}SH$, namely, -1.0 V (Fig. 7). Under these conditions, the highest coverage with thiols is attained after 10 min polarization of the electrode, at the modifier concentrations, 12.5 μM for C_4A-$(SH)_4$ and 30 μM for $C_{11}SH$, in the solution. Compared to the self-assembly process, the optimum adsorption concentrations of both the compounds are lower. Nevertheless, compared to self-assembly, a longer adsorption time is required in the case of $C_{11}SH$ potential-assisted deposition from NaOH to attain the highest surface coverage.
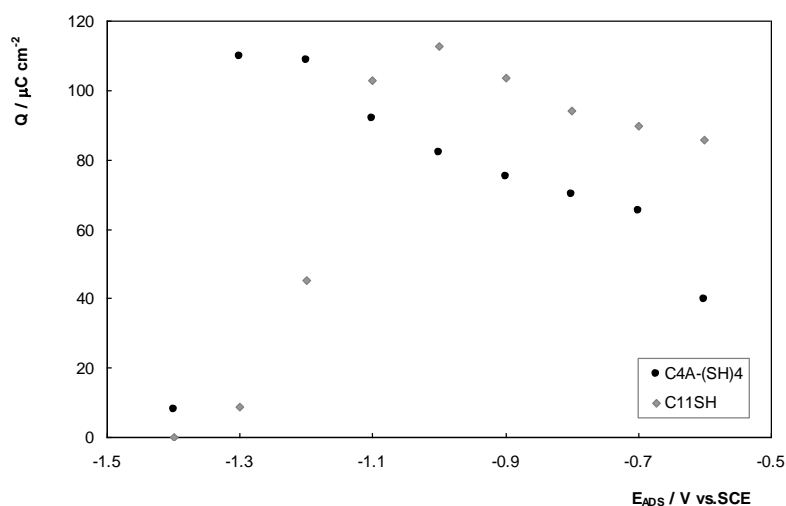
Figure 7. Dependences of the modified electrode charge on the adsorption potential of C_4A-$(SH)_4$ and $C_{11}SH$ (deposition: t_{ADS} 300 s; $C_{11}SH$: c_{ADS} 30 μM, C_4A-$(SH)_4$: c_{ADS} 12.5 μM; CV: $E_{In} = E_{ADS}$; $E_H = -0.5$ V; $E_L = -1.5$ V, scan rate 0.1 V·s^{-1}; base electrolyte: 0.1 M NaOH in a 1:1 mixture of ethanol and water).

Our results for the optimum adsorption potential are in disagreement with the study by Rohwerder et al. [18], where the rate of thiol adsorption decreases with increasing cathodic potentials (the process is faster at positive potentials) and the fully covered electrode surface is attained at negative deposition potentials after about 2000 s. It could indicate an influence of the pH. Our results have been obtained in the alkaline 0.1 M NaOH (1:1) water-ethanolic solution, the work [18] has been carried out in a neutral 0.1 M LiClO$_4$ ethanolic solution.

The desorption charge of the electrode surface fully covered with C$_{11}$SH (Table 1) is about 140 μC cm^{-2} (similar to that of the self-assembly modified electrode, 146 μC cm^{-2}) and corresponds to the results of Phong et al. [81] and to the results obtained from a pressure-area isotherm [78]. The desorption charge of the electrode modified with C$_4$A-(SH)$_4$ by the electrochemical procedure in the NaOH solution is somewhat lower (234 μC cm^{-2}), compared to the self-assembly process.

In comparison with these results, some differences have been observed for the electrode modification in the LiClO$_4$ ethanolic solution at positive electrode potentials. The optimum adsorption times are shorter, 5 min. for the C$_{11}$SH molecule, and 60 s for the C$_4$A-(SH)$_4$ one. However, higher modifier concentrations are required, compared to the electrodeposition from the NaOH solution and to the self-assembly process. The thiol reduction peaks decrease at longer adsorption times and the C4A-(SH)4 reduction peak disappears completely after a 5 min. electrodeposition. This can be caused by formation of oxides on the electrode surface.

Table 1. The optimum adsorption conditions and the resultant coverage of the polycrystalline gold electrodes modified by C$_4$A-(SH)$_4$ and C$_{11}$SH from different solutions and by different techniques of modification.

	Potential-assisted deposition				Self-assembly modification	
	NaOH		LiClO$_4$			
	C$_{11}$SH	C$_4$A-(SH)$_4$	C$_{11}$SH	C$_4$A-(SH)$_4$	C$_{11}$SH	C$_4$A-(SH)$_4$
c$_{ADS}$ (μM)	30.0	12.5	100.0	50.0	50.0	50.0
E$_{ADS}$ (V)	-1.0	-1.3	0.3	0.3	—	—
t$_{ADS}$ (s)	600	600	300	60	180	600
Q (μC cm^{-2})	140	234	89	1063	146	295
A$_{molec}$ (nm^2) *	0.12	0.27	0.18	0.06	0.11	0.22

* The surface area of the electrode corresponding to one modifier molecule

The optimum adsorption potential is 0.3 V for both the thiol compounds. Large differences have been observed in the desorption charge of the modified electrode in comparison with the above results (self-assembly and potential-controlled process in the alkaline solution). Whereas the

desorption   charge   of   the C_4A-$(SH)_4$ modified   electrode   is
1063 μC cm^{-2}, that of the $C_{11}SH$ modified electrode is one order of magnitude lower, i.e. 89 μC cm^{-2}
(the same way of modification, the optimum conditions). Compared to the above results, the value for
the C_4A-$(SH)_4$ modified electrode is almost four times higher. On the other hand, the charge of the
$C_{11}SH$ modified electrode is almost one half of that obtained after the modification by the
self-assembly and by potential controlled deposition in the NaOH solution. The results for the
modified electrode desorption charge, as well as the surface areas per thiol molecule, coming from the
electrode charge, much differ from those discussed with the previous two processes and from the
conclusions based on the pressure-area isotherms [78-80]. This indicates the formation of disordered
thiol layers. Therefore, the potential-assisted electrode modification from the $LiClO_4$ ethanolic solution
is found to be inconvenient for creation of well-defined and reproducible surface-modifying layers.

3.4. Cyclic voltammetry measurements in redox systems
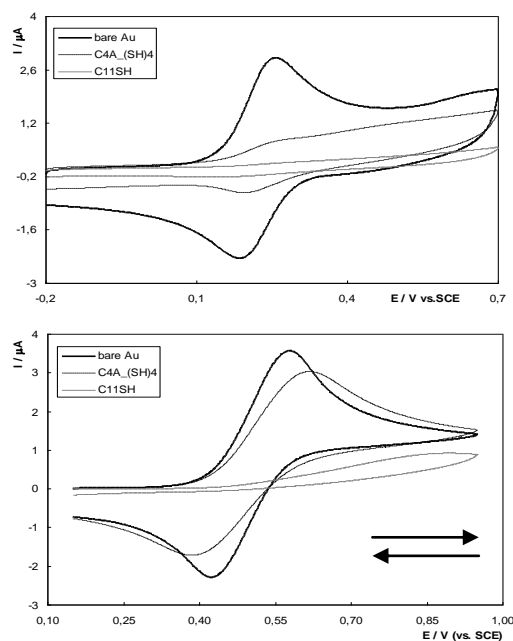
Figure 8. Cyclic voltammetric curves at a bare polycrystalline Au disk electrode (solid line) and at a
calixarene (dotted line) and undecanethiol (gray solid line) modified electrode with A) 1 mM
$K_4[Fe(CN)_6]$ in the 0.5 M acetate buffer (E_{In} = -0.2 V, E_H = 0.7 V, v = 0.1 V·s^{-1}) and B) with
1 mM ferrocene in 10 mM Bu_4NPF_6 dissolved in nitrobenzene (E_{In} = -0.15 V, E_H = 0.95 V,
v = 0.05 V·s^{-1}). Modified electrodes: Self-assembly modification (c_{ADS} 5·10^{-5} M DMF solution;
t_{ADS} 10 min for both compounds).

The electrochemical properties of the adsorbed layers have been studied in an inorganic
aqueous system of 0.5 M acetate buffer, using potassium ferrocyanide ($K_4[Fe(CN)_6]$) (Fig. 8A) and in
an organic phase containing ferrocene (Fig. 8B) as electrochemical probes. The results have been

compared with those obtained on a bare polycrystalline gold electrode. Using the bare electrode (Fig. 8A, solid line), the cyclic voltammograms exhibit the typical reversible oxidation and reduction peaks between potentials of 0 and 0.4 V vs. SCE. The oxidation peak close to 1.0 V, and the reduction peak close to 0.7 V correspond to the gold oxide formation. The redox reaction of $Fe(CN)_6^{3-}$ / $Fe(CN)_6^{4-}$ on the C_4A-$(SH)_4$ modified electrode is discussed in our previous study [49]; the reaction is irreversible. Compared to this, the reaction does not occur at all on the $C_{11}SH$ modified layer. The electrode surface is completely covered by the $C_{11}SH$ molecules and the layer, which behaves as an insulator, prohibits the electrode reaction.

The electrochemical behavior of the modified electrodes in the organic phase in the presence of ferrocene has a similar character (Fig. 8B). The thiol layer also changes the reversibility of the redox system. On the C_4A-$(SH)_4$ layer, both the ferrocene oxidation and reduction peaks are observed on the CV curve, but the distance between them is prolonged. The C_4A-$(SH)_4$ layer makes the reaction with the gold surface more difficult, but the reaction is not suppressed completely. On the $C_{11}SH$ modified layer, a slight oxidation reaction is observed close to a potential of 0.85 V vs. Ag/ AgCl electrode, but no opposite reduction peak is observed. The $C_{11}SH$ layer actually also behaves as an insulator in this redox system.

4. CONCLUSIONS

The study of the differences in the thiol reduction desorption processes for $C_{11}SH$ and C_4A-$(SH)_4$ bonding to a polycrystalline gold electrode indicates that the main reduction peak of the linear chain $C_{11}SH$ appears at a more positive potentials, compared to that of C_4A-$(SH)_4$. This can possibly be utilized in future studies of mixed layers of both the thiol compounds. However, the crystallographic orientation of the polycrystalline gold and the terraced surface make the desorption process more difficult and smaller peaks appear prior to the main reduction peaks with both the thiols.

In the case of $C_{11}SH$, the free desorbed molecules are subsequently adsorbed back on the electrode surface and this process is faster than the diffusion of the molecules into the solution. This effect is more pronounced with $C_{11}SH$, because in the desorption of C_4A-$(SH)_4$, the peak obtained on the second reduction scan is by 96 % smaller than that obtained on the first scan. The impedance measurements of the double layer capacity have confirmed that the modifier layers are stable: the $C_{11}SH$ layer behaves as an insulator within a potential range from -0.2 to -0.9 V; the layer is fully desorbed at a potential of -1.3 V. The C_4A-$(SH)_4$ layer forms a barrier on the electrode surface, which is stable up to a potential of -1.40 V. Nevertheless, the C_4A-$(SH)_4$ layer is not as compact as that of $C_{11}SH$. This conclusion has been confirmed by the measurement in redox systems, where the $C_{11}SH$ layer behaves as an insulator and the redox reactions are almost fully suppressed. On the other hand, the C_4A-$(SH)_4$ layer forms a barrier on the electrode surface which can be penetrated by the electroactive molecule, but the reaction is slowed down in comparison with the bare electrode.

Three ways of modification of a polycrystalline gold electrode have been compared in the next step. The optimum adsorption conditions and the charges on the modified electrodes (corresponding to the coverage of the electrodes), summarized in Table 1, indicate that identical modifier layers are attained by the self-assembly process and by the thiol electrodeposition from 0.1 M NaOH solution at negative potentials. For the preparation of a mixed layer of both the thiol compounds, the electrochemical deposition from 0.1 M NaOH seems to be more suitable and simpler. A layer of C_4A-$(SH)_4$ would be created at a potential of -1.3 V and then any defects would be filled up at a potential of -1.0 V by the deposition of $C_{11}SH$ molecules.

The calculation of the gold surface area per molecule for both the compounds indicates that the compact $C_{11}SH$ layer is formed on the electrode surface. On the other hand, the area per C_4A-$(SH)_4$ molecule is lower, compared to the literature values for similar molecules. However, the cause of this observation most probably lies in the fact that the uneven surface of the polycrystalline gold does not permit bonding of the C_4A-$(SH)_4$ molecules by all the four –SH groups, compared to $C_{11}SH$ containing a single –SH group. The C_4A-$(SH)_4$ molecules do not form compact layers on the uneven surface - see the penetration of the background electrolyte ions observed in the capacity measurements, or the less pronounced suppression of redox reactions.

The utilization of a modified polycrystalline gold electrode for designing a specific sensor is possible, but the complicated crystallographic structure and the consequent roughness of the surface may substantially complicate the modifying process. These problems are more pronounced with layers of large molecules containing a greater number of bounding groups, such is C_4A-$(SH)_4$ in the present work. Therefore, gold single-crystal electrodes are substantially more promising.

References

1. L. Becucci, R. Guidelli, C. Peggion, C. Toniolo and M. R. Moncelli, *Journal of Electroanalytical Chemistry*, 576 (2005) 121.
2. L. Becucci, M. Innocenti, E. Salvietti, A. Rindi, I. Pasquini, M. Vassalli, M. L. Foresti and R. Guidelli, *Electrochimica Acta*, 53 (2008) 6372.
3. L. Becucci, M. R. Moncelli, R. Naumann and R. Guidelli, *Journal of the American Chemical Society*, 127 (2005) 13316.
4. B. Genorio, T. He, A. Meden, S. Polanc, J. Jamnik and J. M. Tour, *Langmuir*, 24 (2008) 11523.
5. C. M. Ruan, T. Bayer, S. Meth and C. N. Sukenik, *Thin Solid Films*, 419 (2002) 95.

6.   D. Garcia-Raya, R. Madueno, J. M. Sevilla, M. Blazquez and T. Pineda, *Electrochimica Acta*, 53 (2008) 8026.
7.   P. Gupta, K. Loos, A. Korniakov, C. Spagnoli, M. Cowman and A. Ulman, *Angewandte Chemie-International Edition*, 43 (2004) 520.
8.   R. Colorado Jr, T. R. Lee, K. H. J. Buschow, W. C. Robert, C. F. Merton, I. Bernard, J. K. Edward, M. Subhash and V. Patrick, in Encyclopedia of Materials: Science and Technology, Elsevier, Oxford, 2001, p. 9332.
9.   D. Mandler and I. Turyan, *Electroanalysis*, 8 (1996) 207.
10. M. Cohen-Atiya and D. Mandler, *Journal of Electroanalytical Chemistry*, 550-551 (2003) 267.
11. A. Ulman, *Chemical Reviews*, 96 (1996) 1533.
12. S. Chon and W. K. Paik, *Physical Chemistry Chemical Physics*, 3 (2001) 3405.
13. W. K. Paik, S. Eu, K. Lee, S. Chon and M. Kim, *Langmuir*, 16 (2000) 10198.
14. F. Y. Ma and R. B. Lennox, *Langmuir*, 16 (2000) 6188.
15. R. Meunier-Prest, G. Legay, S. Raveau, N. Chiffot and E. Finot, *Electrochimica Acta*, 55 (2010) 2712.
16. R. G. Pillai, M. D. Braun and M. S. Freund, *Langmuir*, 26 (2010) 269.
17. S. Rifai, M. Laferriere, D. Qu, D. D. M. Wayner, C. P. Wilde and M. Morin, *Journal of Electroanalytical Chemistry*, 531 (2002) 111.
18. M. Rohwerder, K. de Weldige and M. Stratmann, *Journal of Solid State Electrochemistry*, 2 (1998) 88.
19. H. Ron and I. Rubinstein, *Journal of the American Chemical Society*, 120 (1998) 13444.
20. R. G. Pillai and M. S. Freund, *Langmuir*, 27 (2011) 9028.
21. B. Sustrova, V. Marecek and K. Stulik, in Modern Electrochemical Methods XXXI, BEST Servis, Ústí nad Labem, Jetřichovice, 2011, p. 153.
22. I. Sestakova and T. Navratil, *Bioinorganic Chemistry and Applications*, 3 (2005) 43.
23. J. Fischer, L. Vanourkova, A. Danhel, V. Vyskocil, K. Cizek, J. Barek, K. Peckova, B. Yosypchuk and T. Navratil, *International Journal of Electrochemical Science*, 2 (2007) 226.
24. S. Sebkova, T. Navratil and M. Kopanica, *Analytical Letters*, 38 (2005) 1747.
25. L. Vankova, L. Maixnerova, K. Cizek, J. Fischer, J. Barek, T. Navratil and B. Yosypchuk, *Chemicke Listy*, 100 (2006) 1105.
26. K. Peckova, J. Barek, T. Navratil, B. Yosypchuk and J. Zima, *Analytical Letters*, 42 (2009) 2339.
27. V. Vyskocil, T. Navratil, P. Polaskova and J. Barek, *Electroanalysis*, 22 (2010) 2034.
28. Z. Dlaskova, T. Navratil, M. Heyrovsky, D. Pelclova and L. Novotny, *Analytical and Bioanalytical Chemistry*, 375 (2003) 164.
29. D. Cabalkova, J. Barek, J. Fischer, T. Navratil, K. Peckova and B. Yosypchuk, *Chemicke Listy*, 103 (2009) 236.
30. V. Vyskocil, T. Navratil, A. Danhel, J. Dedik, Z. Krejcova, L. Skvorova, J. Tvrdikova and J. Barek, *Electroanalysis*, 23 (2011) 129.
31. K. Peckova, T. Navratil, B. Yosypchuk, J. C. Moreira, K. C. Leandro and J. Barek, *Electroanalysis*, 21 (2009) 1750.
32. J. Barek, D. Cabalkova, J. Fischer, T. Navratil, K. Peckova and B. Yosypchuk, *Environmental Chemistry Letters*, 9 (2011) 83.
33. K. Novakova, T. Navratil, J. Jaklova Dytrtova and J. Chylkova, *International Journal of Electrochemical Sciences* (2012) Accepted.
34. M. Masarik, J. Gumulec, M. Sztalmachova, M. Hlavna, P. Babula, S. Krizkova, M. Ryvolova, M. Jurajda, J. Sochor, V. Adam and R. Kizek, *Electrophoresis*, 32 (2011) 3576.

35. T. Navratil, S. Sebkova and M. Kopanica, *Analytical and Bioanalytical Chemistry*, 379 (2004) 294.
36. T. Navratil, B. Yosypchuk and J. Barek, *Chemia Analityczna (Warsaw)*, 54 (2009) 3.
37. Z. Dlaskova, T. Navratil, L. Novotny, D. Pelclova and P. Madlova, *Chemicke Listy*, 93 (1999) 142.
38. T. Navratil, Z. Dlaskova, M. Kopanica and L. Novotny, *Chemicke Listy*, 95 (2001) 127.
39. T. Navratil and M. Kopanica, *Critical Reviews in Analytical Chemistry*, 32 (2002) 153.
40. T. Navratil and M. Kopanica, *Chemicke Listy*, 96 (2002) 111.
41. I. Sestakova, J. Jaklova Dytrtova, M. Jakl and T. Navratil, *International Journal of Energy and Environment*, 5 (2011) 347.
42. S. Sander, T. Navratil, P. Basova and L. Novotny, *Electroanalysis*, 14 (2002) 1133.
43. S. Sander, T. Navratil and L. Novotny, *Electroanalysis*, 15 (2003) 1513.
44. J. Sochor, O. Zitka, D. Hynek, E. Jilkova, L. Krejcova, L. Trnkova, V. Adam, J. Hubalek, J. Kynicky, R. Vrba and R. Kizek, *Sensors*, 11 (2011) 10638.
45. D. Hynek, J. Prasek, J. Pikula, V. Adam, P. Hajkova, L. Krejcova, L. Trnkova, J. Sochor, M. Pohanka, J. Hubalek, M. Beklova, R. Vrba and R. Kizek, *International Journal of Electrochemical Science*, 6 (2011) 5980.
46. T. Navratil, *Current Organic Chemistry*, 15 (2011) 2996.
47. T. Navratil, M. Kopanica and J. Krista, *Chemia Analityczna (Warsaw)*, 48 (2003) 265.
48. B. Sustrova, V. Marecek and K. Stulik, in T. Navratil, J. Barek (Editors), Modern Electrochemical Methods XXX, 2010, p. 172.
49. B. Sustrova, K. Stulik, V. Marecek and P. Janda, *Electroanalysis*, 22 (2010) 2051.
50. T. Navratil, I. Sestakova, V. Marecek and K. Stulik, in J. Barek, T. Navratil (Editors), Modern Electrochemical Methods XXX, BEST Servis, Jetrichovice, 2010, p. 119.
51. T. Navratil, I. Sestakova and V. Marecek, *International Journal of Electrochemical Science*, 6 (2011) 6032.
52. T. Navratil, I. Sestakova, J. Jaklova Dytrtova, M. Jakl and V. Marecek, *WSEAS Transactions on Environment and Development*, 6 (2010) 208.
53. T. Navratil, I. Sestakova and V. Marecek, in V. Mladenov, K. Psarris, N. Mastorakis, A. Caballero, G. Vachtsevanos (Editors), Development, Energy, Environment, Economics (DEEE '10), Puerto de la Cruz, 2010, p. 192.
54. T. Navratil, I. Sestakova and V. Marecek, *International Journal of Energy and Environment*, 5 (2011) 337.
55. M. Parisova, I. Sestakova, T. Navratil and V. Marecek, in T. Navratil, M. Fojta (Editors), Modern Electrochemical Methods XXXII, BEST servis, Jetrichovice, 2012, p. 102.
56. T. Navratil, I. Sestakova and V. Marecek, in T. Navratil, J. Barek (Editors), Modern Electrochemical Methods XXXI, BEST Servis, Jetrichovice, 2011, p. 91.
57. T. Navratil, I. Sestakova, J. Jaklova Dytrtova, M. Jakl and V. Marecek, in M. Otesteanu, S. Celikyay, N. Mastorakis, S. Lache, F.K. Benra (Editors), 7th WSEAS International Conference on Environment, Ecosystems and Development, World Scientific and Engineering Acad. and Soc., Puerto de la Cruz, SPAIN, 2009, p. 212.
58. J. Jaklova Dytrtova, M. Jakl, T. Navratil and D. Schroder, *Collection of Czechoslovak Chemical Communications*, 76 (2011).
59. M. Parisova, T. Navratil, I. Sestakova, J. Jaklova Dytrtova and V. Marecek, *International Journal of Electrochemical Science* (2012) Accepted.
60. J. Jaklova Dytrtova, M. Jakl, I. Sestakova, E. L. Zins, D. Schroder and T. Navratil, *Analytica Chimica Acta*, 693 (2011) 100.

61. T. Navratil, I. Sestakova, K. Stulik and V. Marecek, *Electroanalysis*, 22 (2010) 2043.
62. J. Jaklova Dytrtova, I. Sestakova, M. Jakl and T. Navratil, *Electroanalysis*, 21 (2009) 573.
63. D. Huska, O. Zitka, O. Krystofova, V. Adam, P. Babula, J. Zehnalek, K. Bartusek, M. Beklova, L. Havel and R. Kizek, *International Journal of Electrochemical Science*, 5 (2010) 1535.
64. P. Majzlik, A. Strasky, V. Adam, M. Nemec, L. Trnkova, J. Zehnalek, J. Hubalek, I. Provaznik and R. Kizek, *International Journal of Electrochemical Science*, 6 (2011) 2171.
65. V. Shestivska, V. Adam, J. Prasek, T. Macek, M. Mackova, L. Havel, V. Diopan, J. Zehnalek, J. Hubalek and R. Kizek, *International Journal of Electrochemical Science*, 6 (2011) 2869.
66. O. Zitka, H. Skutkova, O. Krystofova, P. Sobrova, V. Adam, J. Zehnalek, L. Havel, M. Beklova, J. Hubalek, I. Provaznik and R. Kizek, *International Journal of Electrochemical Science*, 6 (2011) 1367.
67. D. Hynek, L. Krejcova, J. Sochor, N. Cernei, J. Kynicky, V. Adam, L. Trnkova, J. Hubalek, R. Vrba and R. Kizek, *International Journal of Electrochemical Science*, 7 (2012) 1802.
68. L. Krejcova, I. Fabrik, D. Hynek, S. Krizkova, J. Gumulec, M. Ryvolova, V. Adam, P. Babula, L. Trnkova, M. Stiborova, J. Hubalek, M. Masarik, H. Binkova, T. Eckschlager and R. Kizek, *International Journal of Electrochemical Science*, 7 (2012) 1767.
69. M. Pohanka, M. Hrabinova, J. Fusek, D. Hynek, V. Adam, J. Hubalek and R. Kizek, *International Journal of Electrochemical Science*, 7 (2012) 50.
70. P. Sobrova, M. Ryvolova, D. Huska, J. Hubalek, I. Provaznik, V. Adam and R. Kizek, *International Journal of Electrochemical Science*, 7 (2012) 1.
71. P. Sobrova, M. Ryvolova, D. Hynek, V. Adam, J. Hubalek and R. Kizek, *International Journal of Electrochemical Science*, 7 (2012) 928.
72. A. Kleckerova, P. Sobrova, O. Krystofova, J. Sochor, O. Zitka, P. Babula, V. Adam, H. Docekalova and R. Kizek, *International Journal of Electrochemical Science*, 6 (2011) 6011.
73. J. J. Calvente, G. Lopez-Perez, J. M. Jurado, R. Andreu, M. Molero and E. Roldan, *Langmuir*, 26 (2010) 2914.
74. C. Buess-Herman, T. Doneux, M. Steichen and A. De Rache, *Journal of Electroanalytical Chemistry*, 649 (2010) 164.
75. M. S. El-Deab and T. Ohsaka, *Electrochimica Acta*, 49 (2004) 2189.
76. D. M. Lemay and J. L. Shepherd, *Electrochimica Acta*, 54 (2008) 388.
77. M. M. Walczak, C. A. Alves, B. D. Lamp and M. D. Porter, *Journal of Electroanalytical Chemistry*, 396 (1995) 103.
78. D. Vollhardt, V. B. Fainerman and G. Emrich, *Journal of Physical Chemistry B*, 104 (2000) 8536.
79. M. W. Sugden, T. H. Richardson, F. Davis, S. P. J. Higson and C. F. J. Faul, *Colloids and Surfaces A: Physicochemical and Engineering Aspects*, 321 (2008) 43.
80. K. Yagi, S. B. Khoo, M. Sugawara, T. Sakaki, S. Shinkai, K. Odashima and Y. Umezawa, *Journal of Electroanalytical Chemistry*, 401 (1996) 65.
81. P. H. Phong, H. Tomono, N. Nishi, M. Yamamoto and T. Kakiuchi, *Electrochimica Acta*, 53 (2008) 4900.